ResearchGate

See discussions, stats, and author profiles for this publication at: https://www.researchgate.net/publication/51466461

# Fluoroalkyl-Functionalized Silica Particles: Synthesis, Characterization, and Wetting Characteristics

**ARTICLE** *in* LANGMUIR · AUGUST 2011

Impact Factor: 4.46 · DOI: 10.1021/la201545a · Source: PubMed

CITATIONS
26

READS
73

**4 AUTHORS**, INCLUDING:

Raymond Campos
University of Texas at Dallas
**11** PUBLICATIONS **84** CITATIONS
SEE PROFILE

Andrew J. Guenthner
Air Force Research Laboratory
**98** PUBLICATIONS **682** CITATIONS
SEE PROFILE

Joseph Mark Mabry
Air Force Research Laboratory
**141** PUBLICATIONS **3,033** CITATIONS
SEE PROFILE

Available from: Andrew J. Guenthner
Retrieved on: 03 February 2016

Langmuir

ARTICLE

pubs.acs.org/Langmuir

# Fluoroalkyl-Functionalized Silica Particles: Synthesis, Characterization, and Wetting Characteristics

Raymond Campos,[†] Andrew J. Guenthner,[‡] Timothy S. Haddad,[†] and Joseph M. Mabry*[,‡]

[†]ERC, Inc., Space & Missile Propulsion Division, Air Force Research Laboratory, Edwards AFB, California 93524, United States

[‡]Space & Missile Propulsion Division, Air Force Research Laboratory, Edwards AFB, California 93524, United States

Supporting Information

**ABSTRACT:** Fluoroalkyl-functionalized silica particles for use in nonwetting surfaces were prepared by treatment of silica particles with fluoroalkyl-functional chlorosilanes. Both fumed and precipitated silica were studied, as well as the efficiency of surface coverage using mono-, di-, and trifunctional chlorosilanes. The most effective surface treatment was accomplished via the surface grafting of monofunctional chlorosilanes in the presence of preadsorbed dimethylamine under anhydrous conditions at room temperature. Confirmation of covalent attachment was accomplished via Fourier transform infrared (FT-IR) spectroscopy, while elemental analysis, thermogravimetric analysis, and nitrogen adsorption isotherms were used to determine grafting densities and additional key geometric characteristics of the grafted layer. The effect of residual silanol content on the moisture uptake properties of the modified silica particles was determined by measuring the water uptake of unbound particles, while liquid wetting properties were determined by dynamic contact angle analysis of elastomeric composites. Although residual silanol content was shown to effect wetting properties, results suggest that surface geometry dominates the performance of liquid-repellent surfaces. The potential use of fluoroalkyl-functionalized silica particles for hydrophobic and oleophobic applications is discussed.

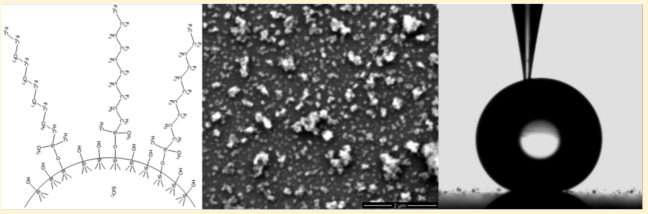

## INTRODUCTION

The field of liquid-repellant surfaces has experienced a recent surge in interest due to new revelations about the contributions of surface energy and geometry to imparting resistance to wetting.[1−7] Strict control of key parameters has enabled the production of nonwetting surfaces that can repel droplets of water as well as liquids with significantly lower surface tension values, such as alkanes and alcohols. The desire for both low surface energy values and appropriate surface morphology has resulted in a wide variety of synthetic methodologies for attaining desired properties. Methods to achieve appropriate surface morphology include etching,[8−11] electrospinning,[12−14] lithography,[13,14] spraying,[15−17] and particle impregnation.[18] The use of materials with inherent texture, such as textiles, has also been employed,[6,19,20] with the low surface-energy requirement typically being met from a fluorine-containing polymer,[18,21] silane,[11,12,22] or crystalline-solid.[6,13,14,19,20] However, a simple and affordable method that can be used to produce durable nonwetting surfaces remains one of the key challenges in producing useful superhydrophobic and superoleophobic surfaces.

Functionalized silica particles in combination with a fluoropolymer matrix are one way to achieve extended durability for a wide range of hydrophobic surface coatings.[23,24] In addition, composite coatings with high silica particle content have been shown to possess a hierarchical morphology, with nanoscale features formed by primary particles and porous micrometer-sized features formed by aggregates.[15,25] Thus, when silica particles are embedded into surfaces, multiple scales of roughness and re-entrant curvature are likely to result, and it is precisely these two features that have been recently attributed to extreme nonwetting behavior.[1−6]

The modification of silica particles via substitution of surface silanol groups with mono- or multifunctional silanes has proven to be a reliable approach to achieving satisfactory surface coverage of desired functional groups, while preserving the high specific surface area of the silica particles.[26−29] Fluoroalkyl-functionalized silica particles have demonstrated both low surface energy and compatibility with fluorine-containing polymer matrices.[30] Surfaces produced using these materials have been utilized primarily in chromatographic applications,[29,31−34] though some investigations involving resistance to wetting by water and other liquids have also been performed.[18,25,35−37]

Although these modified silica particles would seem a natural choice for invoking desirable nonwetting characteristics, there are numerous issues relating to the chemical modification of these particles that could significantly affect their performance. For instance, reported silanol group densities vary widely on silica surfaces, with measurements ranging from 4 to 12 silanols/nm$^2$.[38,39] This silanol density is dependent on the method of

**Received:** April 26, 2011
**Revised:** June 24, 2011
**Published:** July 05, 2011

ACS Publications © 2011 American Chemical Society

**Table 1. Summary of Fluoroalkyl-Functionalized Silica**

| sample | silica | silane | method |
|---|---|---|---|
| Fum-Blank | fumed, 7 nm | none | 1 |
| Fum-FPro-MCS | fumed, 7 nm | (3,3,3-trifluoropropyl)dimethylchlorosilane | 1 |
| Fum-FOct-MCS | fumed, 7 nm | (1H,1H,2H,2H-perfluorooctyl)dimethylchlorosilane | 1 |
| Fum-FDec-MCS | fumed, 7 nm | (1H,1H,2H,2H-perfluorodecyl)dimethylchlorosilane | 1 |
| Prec-Blank | precipitated, 22 nm | none | 1 |
| Prec-FPro-MCS | precipitated, 22 nm | (3,3,3-trifluoropropyl)dimethylchlorosilane | 1 |
| Prec-FOct-MCS | precipitated, 22 nm | (1H,1H,2H,2H-perfluorooctyl)dimethylchlorosilane | 1 |
| Prec-FDec-MCS | precipitated, 22 nm | (1H,1H,2H,2H-perfluorodecyl)dimethylchlorosilane | 1 |
| Prec-FDec-DCS | precipitated, 22 nm | (1H,1H,2H,2H-perfluorodecyl)methyldichlorosilane | 1 |
| Prec-FDec-TCS | precipitated, 22 nm | (1H,1H,2H,2H-perfluorodecyl)trichlorosilane | 1 |
| Prec-FDec-MCS-2 | precipitated, 22 nm | (1H,1H,2H,2H-perfluorodecyl)dimethylchlorosilane | 2 |
| Prec-FDec-MCS-3 | precipitated, 22 nm | (1H,1H,2H,2H-perfluorodecyl)dimethylchlorosilane | 3 |
| Prec-FDec-MCS-4 | precipitated, 22 nm | (1H,1H,2H,2H-perfluorodecyl)dimethylchlorosilane | 4 |

silica manufacture and thermal history as well as on the method used to measure silanol content. A model amorphous silica surface, based on the $\beta$-crystallobite form of crystalline silica, has been previously estimated to contain approximately 4.6 silanols/nm$^2$.[38,40,41] However, reported alkyl grafting densities have not exceeded 2−3 nm$^{-2}$, even when using monofunctional silanes, which enable a possible 1:1 substitution of surface silanols.[34,38,42−46] As a result, a significant number of hydroxyl groups remain on the surface, and though they may be occluded by overlaying material, surface rearrangements induced by contact with probing liquids could allow them to emerge and/or exert an influence on wetting behavior. Additionally, silane architecture, in reference to fluoroalkyl chain length and degree of functionality (i.e., mono-, di-, or trifunctional), will have an effect on the surface energy and subsequent wetting properties. The successful development and application of fluoroalkyl-functionalized silica particles for surfaces with durable nonwetting characteristics, therefore, depends on achieving an improved understanding of the aforementioned phenomena.

The present paper describes the development and characterization of fluoroalkyl-functionalized nanosized silica particles for use as surface energy modifiers in liquid-repellant coatings. For these experiments, a variety of (1,1,2,2-tetrahydroperfluoroalkyl)-chlorosilanes were used to treat both fumed and precipitated silica, with variations in both reaction conditions and silane architecture. The treatments resulted in variable densities of both grafted alkyl chains and residual hydroxyl groups, with optimal grafting densities approaching theoretical maxima. The effects of grafting density, grafted chain length, and residual surface functionality on water vapor uptake, wettability, and suitability for nonwetting polymeric coatings are discussed.

## EXPERIMENTAL SECTION

**Materials.** Precipitated silica (Hi-Sil 233, 22 nm diameter, 135 m$^2$/g surface area) was purchased from PPG Industries. Fumed silica (7 nm diameter, 390 ± 40 m$^2$/g surface area) was purchased from Sigma-Aldrich. Fluorinated silane reagents (heptadecafluoro-1,1,2,2-tetrahydrodecyl)dimethylchlorosilane (fluorodecyl monochlorosilane or FDec-MCS); (tridecafluoro-1,1,2,2-tetrahydrooctyl)dimethylchlorosilane (FOct-MCS); (3,3,3-trifluoropropyl)dimethylchlorosilane (FPro-MCS); (heptadecafluoro-1,1,2,2-tetrahydrodecyl)methyldichlorosilane (fluorodecyl dichlorosilane or FDec-DCS); and (heptadecafluoro-1,1,2,2-tetrahydrodecyl)trichlorosilane (fluorodecyl trichlorosilanes or FDec-TCS) were purchased from Gelest, Inc. 1,3-Dichloro-1,2,2,3,3-pentafluoropropane (AK-225G) was purchased from AGC Chemicals Americas, Inc. Anhydrous dimethylamine was purchased from Aldrich. Viton Extreme ETP-600S fluoroelastomer (a copolymer of ethylene, tetrafluoroethylene, perfluoro(methylvinyl) ether, and bromotetrafluorobutene) was obtained from DuPont. The preceding materials were all used as received from the manufacturer. Reagent grade chloroform was purchased from Aldrich and passed through an activated alumina column prior to use. (Heptadecafluoro-1,1,2,2-tetrahydrodecyl)$_8$Si$_8$O$_{12}$ (fluorodecyl$_8$T$_8$ POSS) was synthesized using a previously reported method.[47]

**Fluoroalkyl Functionalization of Silica Particles.** *Method 1 (Standard Procedure).* The surface functionalization of silica particles was performed using Schlenk line techniques, taking great care to minimize moisture exposure. Silica particles (2 g), in a 250 mL round-bottom flask, were initially dried by heating overnight at 200 °C under dynamic vacuum. The dried silica was allowed to cool to room temperature under vacuum and then stirred under 1 atm of dimethylamine for 17 h. The silica particles were then suspended in 80 mL of dry chloroform. A 4-fold excess of fluoroalkyl-substituted chlorosilane reagent (e.g., 7.00 g FDec-MCS), assuming a maximum grafting density of 4 $\mu$mol/m$^2$,[38,45,48] was then added via syringe. The reaction mixture was allowed to stir for 3 days in a dry nitrogen environment before the fluoroalkyl-functionalized silica particles were recovered by centrifuge and purified by exhaustive Soxhlet extraction in chloroform. The extraction was allowed to proceed for 3 days in a nitrogen environment to ensure the removal of any noncovalently bound chlorosilane-derived species or other surface contaminants. After the extraction process, the particles were dried in a stream of nitrogen, transferred to vials, and dried at 100 °C under dynamic vacuum for approximately 1 h. A typical yield was 2.0−2.5 g of modified silica.

*Method 2 (No Base Used).* The second method for functionalizing the silica surface was analogous to the first method with the omission of the dimethylamine. After drying, the silica was allowed to cool to room temperature. The reaction vessel was then backfilled with nitrogen, followed by the addition of chloroform and fluoroalkyl-substituted chlorosilane. The reaction procedure then continued as described in method 1.

*Method 3 (No Base and No Drying).* The initial drying step and dimethylamine addition were omitted from the first method for the functionalization of the silica surface. The silica particles were first suspended in chloroform "as received", and then treated with modifying chlorosilane as described in method 1.

*Method 4 (No Drying).* The initial drying step was omitted from the first method for functionalizing the silica surface. All subsequent steps were analogous to method 1.

Table 1 summarizes the silane treatment procedures employed including the notation for each reaction along with the corresponding silica and fluoroalkyl-silane reagants.

**Characterization of Bonded Phase.** Carbon, hydrogen, nitrogen, and fluorine elemental analyses were performed by Atlantic Microlabs Inc. Integrated thermogravimetric analysis/mass spectroscopy (TGA-MS) experiments were conducted on a TA Q500 TGA apparatus interfaced with a Pfeiffer-Vacuum Thermostar GSD301 MS system. Samples were heated to 1000 °C at 10 °C/min in a nitrogen or air environment. Fourier transform infrared (FT-IR) spectra were collected on a Nicolet 6700 FT-IR spectrometer equipped with a DRIFT Smart Collector. Samples were diluted in KBr at a concentration of 1 wt %.

**Physical Properties of Modified Silica Particles.** *Nitrogen Physisorption Measurements.* Nitrogen adsorption−desorption isotherm experiments were conducted at 77 K using a Micromeritics ASAP 2020 accelerated surface area and porosimetry system. Samples were initially degassed at 110 °C for 8 h under dynamic vacuum. Surface areas were calculated using Brunauer−Emmett−Teller (BET) equation analysis using a nitrogen cross-sectional area of 16.2 $Å^2$.[49]

*Water Uptake Analysis.* Water uptake of functionalized silica particles was determined by exposing particles to 25 °C/90% RH in a Tenney ETCU series environmental chamber for 24 h and then measuring the weight loss due to water evaporation/desorption using thermogravimetric analysis (TGA; TA Instruments Q5000 IR TGA system). The "wet" samples were heated in a nitrogen environment from room temperature to 100 °C at 10 °C/min, held isothermally for 1 h, and then ramped to 1000 °C at 10 °C/min. Weight loss from room temperature to 100 °C was used for water uptake values, while the weight loss up to 1000 °C was used to determine the thermal stability of the grafted layer and to estimate the graft density.

**Production and Dynamic Contact Angle Analysis of Elastomeric Composites.** Elastomeric composites were produced by dispersing 5 mg/mL of either the selected functionalized silica particles or fluorodecyl POSS into a 5 mg/mL Viton fluoroelastomer solution of 1,3-dichloro-1,2,2,3,3-pentafluoropropane (AK-225G) solvent. Composite mixtures were then spin-coated onto silicon wafers at 900 rpm for 30 s. Dynamic contact angles for the composites were measured using a Dataphysics OCA20 goniometer equipped with a TBU90 tilting stage. Deionized water that was further purified using a Millipore system was used as a probing liquid for contact angle measurements. Advancing contact angles were measured by dispensing a 4 $\mu$L droplet onto a test substrate and then slowly adding water to the droplet through a syringe needle at a rate of 0.2 $\mu$L/s until the droplet advanced on the substrate past 5 $\mu$L. This was immediately followed by removing liquid at the same rate until the droplet receded in order to measure the receding contact angle value. The advancing and receding contact angles were measured with an elliptical fit using Dataphysics droplet fitting software. Three to five experiments were conducted on different areas of each sample with contact angles typically varying by ±2.5°. Roll-off angles were measured by placing a 10 $\mu$L droplet onto the test substrate and then slowly tilting the base unit.

## RESULTS AND DISCUSSION

**Effect of Grafting Reaction Parameters.** Because the ultimate goal of efforts reported herein was to prepare low surface-energy particles for use in liquid-repellant surfaces, preparation conditions that were expected to maximize the grafting density of fluoroalkyl-substituents (and simultaneously minimize residual surface polar groups) were pursued. Chloro-functional silanes were chosen over alkoxy-functional silanes because fluoroalkyl-substituted chlorosilanes have been reported to react directly with surface silanols without the presence of water.[50] This finding is significant because an increased amount of surface water has commonly been reported to promote silanol substitution using chloro- or alkoxy-functional silanes.[51−53] However, conducting the silane treatment in anhydrous conditions should minimize undesired side products caused from self-condensation of hydrolyzed silane molecules. This is especially true in the case of di- and trifunctional silanes, where unpredictable surface products are likely to result from polymerization reactions, resulting in ill-defined surface coverage on the modified silica particles.[41,54] Reports of higher overall silane content with increasing water content when using di- and trifunctional silanes are attributed to increasing oligomer content and not to an increase in silanol substitution associated with the formation of a monolayer.

The preferential use of monofunctional silanes over their di- and trifunctional analogues is supported by vapor-phased physisorption measurements that suggest silica particles treated with trifunctional silanes are more hydrophilic in nature than silica particles treated with monofunctional silanes, due to a higher overall silanol content.[33] Additional silanols would originate from the multifunctional silicon atom that was to connect the fluoroalkyl chain to the substrate. Additional evidence is provided from studies that characterize flat $SiO_2$ substrates treated with mono-, di-, or trifunctional silanes using dynamic contact angle analysis.[54,55] In all cases, surfaces treated with multifunctional silanes result in higher water contact angle hysteresis than those treated with monofunctional silanes, indicative of a surface with more heterogeneity. Such heterogeneity would be consistent with an oligomeric coating with appreciable silanol content rather than a homogeneous monolayer.

An amine was employed to further increase the substitution of surface silanols with fluoroalkyl substituents. The use of an amine has been shown to promote covalent attachment of silane molecules to the silica surface at room temperature in the absence of water.[56−58] In addition, studies that were able to maximize grafting density employed the use of an amine or a silane with amine functionality (silazane).[31−33,38,41,42,44,46,59] Two mechanisms have been previously described to explain this observation. The first mechanism involves formation of a silazane and an aminohydrochloride salt byproduct by a substitution reaction between a chlorsosilane and an amine. This produces a silane with a better leaving group that can subsequently react directly with silanol groups. A similar method has been utilized by researchers who choose to isolate the silazane before treating silica particles.[44,46,60] The second mechanism is a two-step process in which amine molecules hydrogen bond to, or deprotonate, surface silanols, rendering the Si−O group of the silanol more nucleophilic, facilitating substitution of incoming silane molecules. In the present study, amine treatment was conducted prior to the silane treatment using gaseous dimethylamine. This order of operation implies that the second mechanism is favored, but it could also facilitate the first mechanism as well. It is important to note that the use of an amine, or having an amine as a leaving group, has the potential to introduce tightly bound hydrophilic groups to the surface. Removal of these species, as well as any amine salt or silane-derived side products, was the rationale for the lengthy purification procedure employed.

In an attempt to optimize reaction conditions, a comparative screening study was performed, in which the chlorosilane functionality, the presence of physisorbed water, and the use of dimethylamine were varied. The precipitated silica was chosen since it was expected to have the largest concentration of unreacted silanols. Table 2 compares the results from elemental analysis, TGA weight loss, BET surface area, and water uptake

**Table 2. Effect of Grafting Reaction Parameters on Key Properties of Treated Silica Particles**

| sample | wt % C | wt % F | % wt loss (23−200 °C) | % wt loss (200−1000 °C) | BET surface area ($m^2$/g) | BET C constant | water uptake (wt %) |
|---|---|---|---|---|---|---|---|
| Prec-Blank | 1.4 | 0.4 | 4.8 | 5.0 | 123 | 127 | 3.7 |
| Prec-FDec-TCS | 4.1 | 6.6 | 4.3 | 16.1 | 128 | 30 | 3.2 |
| Prec-FDec-DCS | 6.1 | 9.0 | 3.5 | 21.2 | 94 | 23 | 3.0 |
| Prec-FDec-MCS | 5.8 | 9.9 | 3.8 | 20.1 | 92 | 21 | 2.8 |
| Prec-FDec-MCS-2 | 2.7 | 3.8 | 4.7 | 10.0 | 124 | 32 | 4.1 |
| Prec-FDec-MCS-3 | 4.3 | 6.1 | 3.6 | 16.0 | 111 | 27 | 3.2 |
| Prec-FDec-MCS-4 | 4.2 | 2.6 | 7.4 | 12.3 | 108 | 24 | 4.2 |

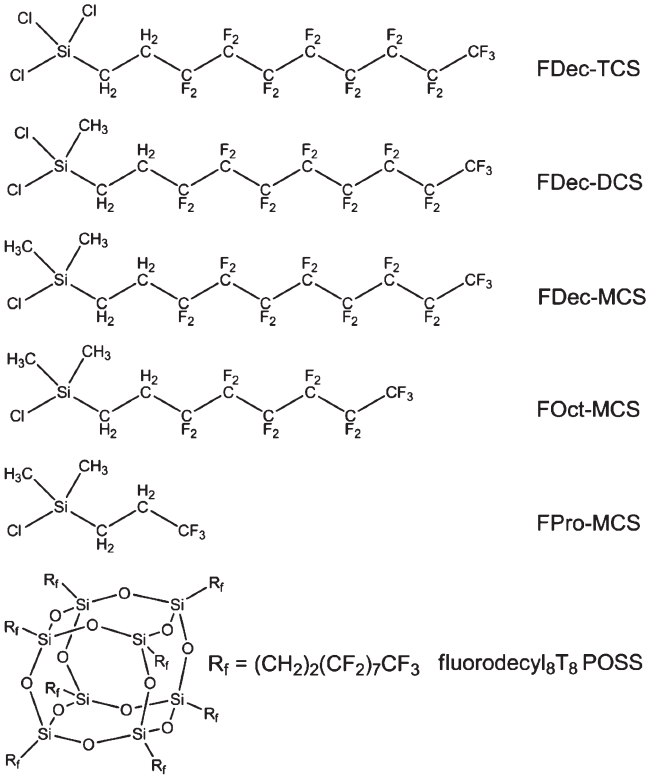


**Figure 1.** Fluorinated materials used in this work.

experiments. The "blank" sample was produced by method 1 with the silane omitted. It should be noted that the BET "C constant" has previously been reported to exhibit a strong correlation with surface energy.[61] The desirable characteristics for hydrophobic materials are a high grafting density (as represented by a high weight percent of F and C, as well as weight loss at 200−1000 °C), a low content of hydrophilic groups (as represented by water uptake, weight loss below 200 °C, which is expected to mainly consist of water and dimethylamine), and a low surface energy (a low BET "C constant"). Maintenance of a reasonably high specific surface area is also considered desirable for liquid-repellant surfaces, as it indicates preservation of the multiscale surface roughness that is desirable for producing a composite solid−liquid−air interface.

Table 2 clearly indicates that either the mono- or dichlorosilane-treated precipitated silica made by method 1 exhibited the most desirable values in each category. The fluorine content was determined to be the most meaningful indicator of coverage, as the silane was expected to be the only available source of fluorine, whereas carbon could arise from a number of sources. Indeed, for the blank sample, the fluorine content was near the lower limit of detection whereas the carbon content was significantly higher. The blank also showed weight loss in the 200−1000 °C range, resulting from condensation of silanols or desorption of strongly bound species. In a similar manner, the water uptake experiment (involving weight loss up to and isothermally at 100 °C after saturation) was judged to be a more significant indicator of potential interference with hydrophobicity than the volatile content of the as-treated particles.

When the aforementioned considerations were taken into account, the monochlorosilane-treated silica produced by method 1 was deemed to be the most desirable for more detailed examination. It should be noted that, based on 9.9 wt % F, the expected carbon content was 1.4 wt % lower than observed and the expected weight loss was 4.6 wt % less than observed, providing the fluorodecyl-dimethylsilyloxyl substituents were the only organic materials on the surface. The additional carbon content and weight loss values were nearly identical to the values found for the blank sample, and in fact all of the samples shown in Table 2 exhibited similar levels of excess carbon and weight loss. Elemental analysis for nitrogen (reported in the Supporting Information) suggest that roughly 1.5 wt % of the sample consisted of residual dimethylamine. This residual material would account for much of the excess carbon, while silanol condensation could account for the additional observed weight loss. Therefore, when calculating silane surface coverage, the fluorine content appeared to be the most reliable basis for computation, rather than the more traditional carbon content or weight loss, which could potentially overestimate the coverage level.

**Effect of Fluoroalkyl Chain Length and Silica Type.** Because monochlorosilanes grafted to the silica surface via method 1 produced the lowest surface energy and highest coverage of fluoroalkylsilane, they were utilized to investigate the effect of silica surface type and fluoroalkyl chain length on the key characteristics of the modified particles. Fluoroalkyl chain lengths of 3, 8, and 10 carbon atoms were chosen, with the two carbon atoms nearest the attachment point being nonfluorinated (see Figure 1). These choices were based on commercial availability and desire to maximize the range of fluorine content.

The key properties for the precipitated silica with varying fluoroalkyl chain lengths are displayed in Table 3, while the corresponding properties for the fumed silica substrate are provided in Table 4. For precipitated silica, all properties show gradual changes with increasing chain length, with the exception of the BET C constant, for which there is a large decrease on silane treatment, with a gradual trend as the chain length is increased. For the fumed silica, the elemental composition and weight loss correspond to silane change according to general expectations, whereas all of the physical properties change

**Table 3. Effect of Fluoroalkyl Chain Length on Key Properties of Treated Precipitated Silica Particles**

| sample | wt % C | wt % F | % wt loss (23−200 °C) | % wt loss (200−1000 °C) | BET surface area ($m^2$/g) | BET C constant | water uptake (wt %) |
|---|---|---|---|---|---|---|---|
| Prec-Blank | 1.4 | 0.4 | 4.8 | 5.0 | 123 | 127 | 3.7 |
| Prec-FPro-MCS | 3.3 | 2.1 | 4.4 | 8.2 | 106 | 29 | 3.4 |
| Prec-FOct-MCS | 5.0 | 7.4 | 4.3 | 16.2 | 101 | 24 | 3.4 |
| Prec-FDec-MCS | 5.8 | 9.9 | 3.8 | 20.1 | 92 | 21 | 2.8 |

**Table 4. Effect of Fluoroalkyl Chain Length on Key Properties of Treated Fumed Silica Particles**

| sample | wt % C | wt % F | % wt loss (23−200 °C) | % wt loss (200−1000 °C) | BET surface area ($m^2$/g) | BET C constant | water uptake (wt %) |
|---|---|---|---|---|---|---|---|
| Fum-Blank | 1.1 | 0.0 | 3.9 | 2.6 | 250 | 111 | 2.9 |
| Fum-FPro-MCS | 5.4 | 4.7 | 1.5 | 9.4 | 256 | 29 | 0.7 |
| Fum-FOct-MCS | 7.9 | 13.4 | 1.0 | 21.3 | 187 | 26 | 0.4 |
| Fum-FDec-MCS | 8.5 | 17.5 | 1.6 | 26.9 | 184 | 25 | 0.6 |

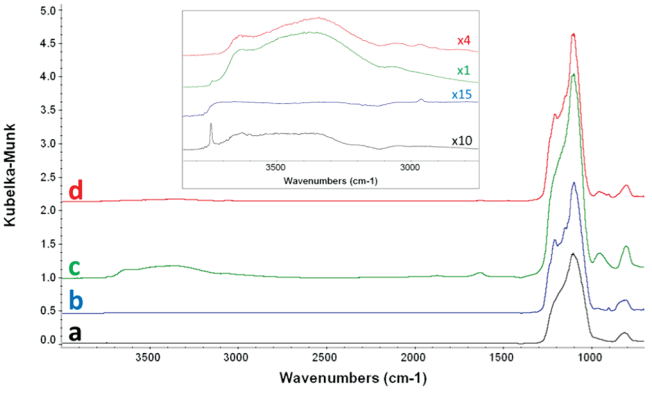


**Figure 2.** Diffuse reflectance infrared spectra of (a) fumed silica, (b) fum-FDec-MCS, (c) precipitated silica, and (d) prec-FDec-MCS.

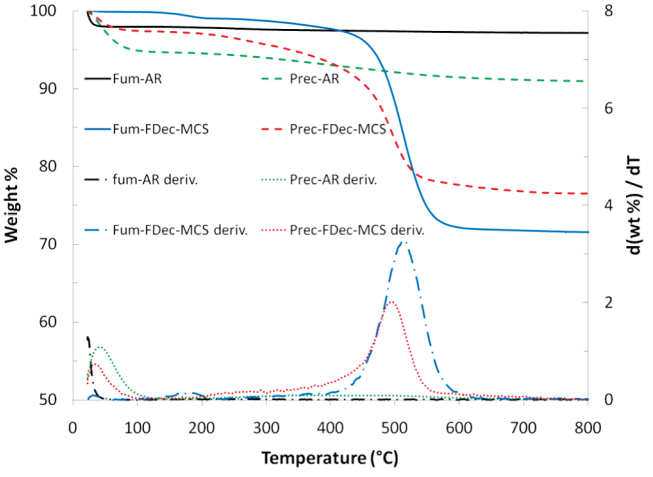


**Figure 3.** Thermogravimetric data for "as received" fumed silica (black solid line), "as received" precipitated silica (green dashed line), FDec-MCS treated fumed silica (blue solid line), and FDec-MCS treated precipitated silica (red dashed lines).

drastically with silane treatment but vary in a more modest and irregular fashion as the grafted chain length increases. The only exception is the BET surface area, which changes drastically on going from three to eight carbon atoms.

Additional insight into the composition of the silica surface was provided by plotting elemental analysis and TGA data as a function of fluoroalkyl chain length or grafted silane molecular weight. The graphs can be seen in Figures S1 and S2 of the Supporting Information along with an in-depth discussion of the graphical analysis.

Graphical analysis indicating the effect of chain length can be summarized as follows. For the precipitated silica, data indicate a constant grafting density along with a small amount of surface contamination. Steadily increasing fluoroalkyl content with increasing chain length resulted in a steady improvement in hydrophobicity. For the fumed silica, there was less surface contamination, and the grafting density appeared to decrease modestly with increasing chain length. Nevertheless, the longer chains imparted slight improvements in characteristics associated with hydrophobicity. In both cases, therefore, the silanes possessing 10 carbon atoms in the fluoroalkyl chain were selected as the most appropriate choice for characterization as superhydrophobic materials.

**Characterization and Model for (1,1,2,2-Tetrahydroperfluorodecyl)dimethylchlorosilane-Treated Silica Surfaces.** The diffuse reflectance infrared Fourier transform (DRIFT) spectra of untreated, "as received", silica and fluorodecyl-dimethylchlorosilane treated silica samples are shown in Figure 2. The strong narrow band at 3747 $cm^{-1}$ in the spectrum for "as received" fumed silica (a) is indicative of isolated silanols on the outer silica surface. This narrow band was significantly weaker in the precipitated silica spectrum (c), consistent with a heavily hydroxylated silica surface with a large population of vicinal and geminal silanols. Broad overlapping peaks from 3000 to 3700 $cm^{-1}$ are attributed to these silanol types, both interior and on the surface, as well as surface adsorbed water. Once silanols are substituted with fluoroalkyl substituents, the isolated silanol band is almost completely absent from spectra for both surface types, indicative of covalent attachment. The formation of siloxane bonds, indicated by the spectral features from 1100 to 1250 $cm^{-1}$, as well as fine stretches in the fingerprint region, also suggests covalent attachment.

Thermogravimetric analysis data for untreated and FDec-MCS treated precipitated and fumed silica can be seen in Figure 3.[62] Untreated, "as received", fumed silica exhibited a modest 2.8%

**Table 5. Estimated Geometric Characteristics of Fluoroalkyl Coatings**

| sample | wt % F | est. grafting density (chains/nm$^2$) | est. coating molar volume (cc) | approx. average coating thickness (nm) | approx. surface area (no overlap) (m$^2$/g) | approx. surface area (3 contacts) (m$^2$/g) | BET surface area (m$^2$/g) |
|---|---|---|---|---|---|---|---|
| Prec-FPro-MCS | 2.1 | 1.7 | 136 | 0.4 | 130 | 120 | 106 |
| Prec-FOct-MCS | 7.4 | 1.5 | 261 | 0.7 | 130 | 110 | 101 |
| Prec-FDec-MCS | 9.9 | 1.6 | 311 | 0.8 | 120 | 100 | 92 |
| Fum-FPro-MCS | 4.7 | 1.4 | 136 | 0.3 | 400 | 300 | 256 |
| Fum-FOct-MCS | 13.4 | 1.1 | 261 | 0.5 | 370 | 240 | 187 |
| Fum-FDec-MCS | 17.5 | 1.2 | 311 | 0.6 | 340 | 190 | 184 |

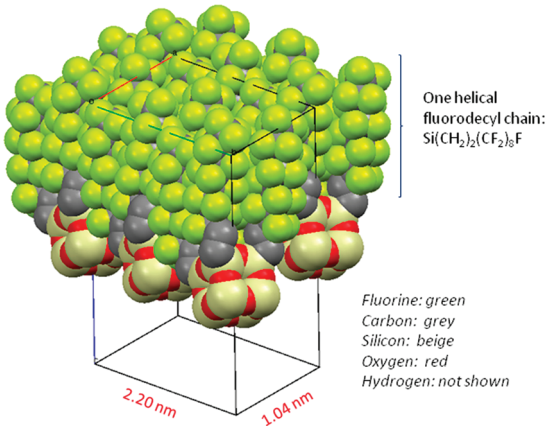


**Figure 4.** Space filling model from the single crystal X-ray structure determination of octa(fluorodecyl)silsesquioxane showing 3.5 fluorodecyl chains/nm$^2$. Three repeat units are displayed with only half the fluorodecyl chains shown.

weight loss from room temperature to 800 °C, while the precipitated silica had a total weight loss of 9.0%. Initial weight loss up to 200 °C is believed to result from the desorption of physically adsorbed water, while the weight loss above 200 °C is mainly attributed to silanol condensation (dehydroxylation). The significantly greater weight loss from the "as received" precipitated silica, particularly between 200 and 800 °C, is consistent with a higher population of silanols compared to that of fumed silica. However, physisorbed water has been reported to outgas beyond 200 °C with isolated silanols remaining beyond 900 °C.[39,63,64] Because of this, overall silanol content can only be roughly estimated from weight loss upon thermal treatment. Treated silica particles display thermal stability up to 400 °C where fluoroalkyl substituents begin to degrade. Mass spectra of the volatiles released at this temperature are consistent with possible fluorine-containing fragments, including hydrofluoric acid. The high thermal stability of the treated silica particles provides additional evidence of covalent attachment and the ability to withstand fluoropolymer processing conditions.

Because both the preparation conditions and the IR spectral data indicate primarily covalent attachment of the fluoroalkylsilane, a physical picture of the treated silica surfaces can be obtained based on the properties shown in Tables 3 and 4. To start, the grafting density (in chains per unit surface area) may be calculated based on the elemental analysis (with the wt % F being the most reliable indicator) and the available surface area. The resultant grafting densities, which range from 1.1 to 1.7 chains/nm$^2$, are listed in Table 5 for the (1,1,2,2-tetrahydroperfluoroalkyl)-dimethylchlorosilane treated silica samples. The grafting densities appear slightly higher for the precipitated silica system and somewhat higher for the shorter fluoroalkyl chains. In all cases, however, the grafting densities are somewhat lower than results reported earlier for fluoroalkylsilane and alkylsilane monolayers (2−3 chains/nm$^2$).[34,38,42−46] However, these grafting densities were calculated exclusively from the carbon content. When using carbon content to calculate grafting density of silane treated silica using method 1, the values increased to between 1.3 and 2.7 nm$^{-2}$ (shown in Table S1 of the Supporting Information). Additionally, one study was found where the grafting density calculated from fluorine content was nearly identical for similarly treated silica using optimal reaction conditions (method 1), ranging from 1.1 to 1.7 nm$^{-2}$, depending on silica type and fluoroalkyl chain-length.[65]

A model for a surface with periodic functionality substituted 100% to form a perfect monolayer is available from the single crystal X-ray structural data for fluorodecyl$_8$T$_8$ POSS.[47] With the basic assumption that this silsesquioxane molecule close packs the fluorodecyl chains in their lowest energy crystal state, the maximum surface coverage attainable for a *perfect* silica surface is 3.5 fluoroalkyl chains/nm$^2$ (Figure 4). The *perfect* packing of fluorodecyl chains on a silica surface is modeled by each unit cell containing 2 molecules with 8 helical fluorodecyl chains crystallizing over an area of 2.28 nm$^2$. Of course, precipitated or fumed silica will never have a perfectly arranged surface of periodic silanols to modify, so coverage less than 3.5 chains/nm$^2$ should be expected.

Although the grafting density values were lower than expected for closely packed monolayers, the surface coverage was not necessarily patchy. A simple tilt of the fluoroalkyl chain axis with respect to the surface would be sufficient to provide complete coverage at a lower grafting density. To investigate this possibility further, the amorphous molar volume of the fluoroalkylsilane (assuming complete hydrolysis) was calculated using the topological correlation described by Bicerano, which is generally accurate to within 5%.[66] The molar volume and grafting density were then used to calculate the approximate average thickness of an amorphous bonded phase coating for each particle (without taking into account overlap). Keeping in mind that a fluoroalkyl chain will typically occupy lateral dimensions of 5−6 Å, the results, shown in Table 5, make clear that there is sufficient grafting density to achieve a high level of surface coverage of the bonded phase, albeit 1−2 layers thick, highly tilted, and likely not well-ordered. The high level of coverage would explain the BET "C constant" values obtained for these samples, which approach those reported for $CF_2$-containing polymers such as Teflon.

**Table 6. Water Contact Angle Measurements of Fluoroelastomer Composites**

| additive | none | Prec FDec-MCS | Fum FDec-MCS | fluorodecyl-POSS |
|---|---|---|---|---|
| loading level (wt %) | | 50 | 50 | 50 |
| $\theta_{adv}/\theta_{rec}$ | 118°/ 86° | 153°/58° | 161°/160° | 121°/115° |

The highly tilted nature of the coverage, which would expose a portion of the nonfluorinated groups in the bonded phase, would also explain why increasing chain length tends to decrease the C constant slightly, as $CF_2$ groups will have a slightly lower surface energy than $CH_2$ groups.

Further evidence for a thin layer of relatively uniform coverage can be found in the BET surface area values of the treated particles. For the as-received particles, the BET surface areas closely match the values expected, based on the reported primary particle size. The blank samples show some decrease in surface area, especially for the fumed silica. The decrease in surface area is attributed to long exposure to basic reaction conditions, causing condensation of silanols in and around pores, as well as in between particle intersections. This "closing off" of pores greatly reduces the accessibility of probing nitrogen molecules, lowering the BET surface area. The degree to which the surface area is decreased during concomitant silane substitution is unclear, but it is assumed to be as great as or lower than the "blank" samples. Using the calculated density and thickness of the coating layer and the reported diameter of the primary particles, an expected value of the specific surface area may be determined. The estimated surface area may be refined somewhat by taking into account the "pinching off" of the surfaces immediately adjacent to interparticle contacts using the geometric formulas for the area of a spherical cap and a reasonable estimate of the number of interparticle contacts (in the case of a porous silica, three contacts per particle). These estimates are also shown in Table 5, where it can be seen that good agreement (given the approximate nature of the calculation) with the reported values, particularly for the precipitated silica, was achieved.

Taken together, the data thus paint a picture of an approximate monolayer of highly tilted fluoroalkyl chains covering the surface of the silica particles. Such a thin, likely disorganized layer would impart dramatically lower surface energy and improve compatibility with fluoropolymers, but it would likely allow small molecules in the vapor phase to pass through and interact with any untreated silanols. Because the reported grafting density is lower than the reported silanol density for both precipitated ($5-12$ silanols/nm$^2$) and fumed ($4-6$ silanols/nm$^2$) silica, there should be a small amount of residual silanol groups on the fumed silica surface and a slightly larger amount on the precipitated silica surface, after treatment. Thus, both the modest reduction in water uptake seen in the precipitated silica and the more significant reduction seen for fumed silica are readily explained by the surface model. The same considerations would also explain why the precipitated silica appeared to retain significantly more surface contaminants than the fumed silica.

**Comparative Characterization of Elastomeric Composites.** Having developed a reasonable model for the treated silica particles, a meaningful comparison to systems containing well-defined fluoroalkyl-substituted silsesquioxane molecules can be undertaken. Surfaces containing fluorodecyl$_8$T$_8$ POSS molecules (Figure 1) are deemed a good comparison for their well-defined nanostructure, which is essentially a model silica particle functionalized with fluorodecyl substituents and no silanol content. As mentioned previously, the silica particles will provide the benefits of compatibility with easily scaled coating processes (such as spray coating), a built-in geometry of multiscale roughness, and greater durability. However, they may pick up moisture and chemical contaminants due to the presence of residual silanol groups. They also feature a surface that is likely more disorganized and consists mainly of $CF_2$ and $CH_2$ groups, as opposed to more ideal fluoroalkyl-substituted silsesquioxanes, in which the surface is likely to consist of well-organized groups with a lower surface energy (similar to that seen for $-CF_3$ groups).

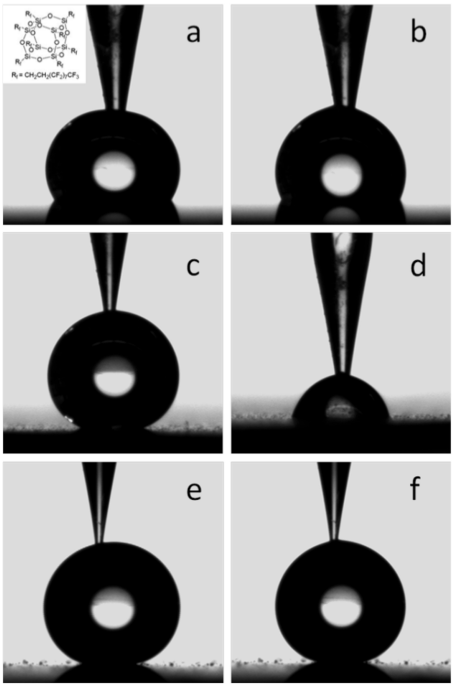


**Figure 5.** Select images of dynamic water contact angle experiments for 50:50 fluoroelastomer/silicate composites: (a) advancing and (b) receding measurements on a fluorodecyl$_8$T$_8$ POSS composite surface; (c) advancing and (d) receding measurements on a prec-FDec-MCS composite surface; and (e) advancing and (f) receding measurements on a fum-FDec-MCS composite surface.

To determine the effects of these potential benefits and drawbacks on liquid repellency, dynamic contact analysis with water droplets was performed on the different materials. Silica samples spin-coated onto glass slides produced static contact angles well over 150° for all modified silica samples.[67] "As received" silica and blank samples completely wet as expected. However, when dynamic experiments were attempted (to measure advancing and receding contact angles), inconclusive results were obtained. Because of the low surface energy of the silica particles, upon adding liquid to a droplet on a modified silica surface, loose silica material could be seen coming off the substrate and into/around the droplet. In some cases, this resulted in the droplet coming into contact with the underlying glass substrate. No definitive trends could be seen when probing samples of varied silica type or silane treatment. This phenomenon is understandable when considering reports of "liquid marbles", where low surface energy particles, such a sub-micrometer oligomeric tetrafluoroethylene (OTFE) particles or

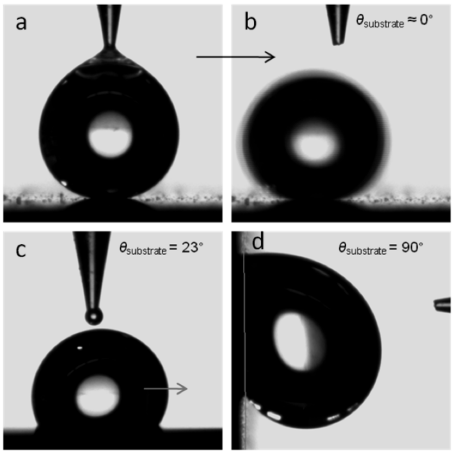


**Figure 6.** Select images exhibiting the wetting behavior of the 50:50 fluoroelastomer/silicate composite surfaces: 5 $\mu$L water droplet (a) before and (b) after detaching from the probing needle onto a fum-FDec-MCS composite surface; (c) 5 $\mu$L water droplet sliding off of a fluorodecyl$_8$T$_8$ composite surface; and (d) 10 $\mu$L water droplet pinned to a prec-FDec-MCS composite surface.

hydrophobized silica, are able to effectively "coat" a droplet of high surface tension water or ionic liquid.[68,69] The silica particles produced in the present study can also be used to produce "liquid marbles".

To mitigate this unwanted behavior, modified silica particles were suspended into mixtures of fluoroelastomer (Viton ETP-600S) in fluorinated solvent (AK-225G) at 50 wt % total solids. The mixtures were then spin-coated onto silicon wafers at 900 rpm for 30 s. For comparison, wafers were spin-coated using the same formulation with fluorodecyl$_8$T$_8$ POSS with a surface roughness well under 100 nm by atomic force microscopy (AFM) and interferometry measurements. Results from the dynamic contact angle experiments can be seen in Table 6 with select images shown in Figure 5. The composite surface containing fluoodecyl$_8$T$_8$ POSS resulted in water $\theta_{adv}/\theta_{rec}$= 121.4 ± 0.5°/115.2 ± 0.5°, consistent with a relatively homogeneous, smooth surface with a high concentration of $CF_2/CF_3$ groups on the surface. The low contact angle hysteresis enables water droplets to easily slide off of the substrate with modest surface tilt. This can be seen in Figure 6a and in Video S1 of the Supporting Information. Composites containing fum-FDec-MCS exhibited superhydrophobic behavior, with $\theta_{adv}/\theta_{rec}$= 160.5 ± 3.5°/160.0 ± 3.4°. This superhydrophobic behavior is indicative of a stable composite solid−liquid−air interface between the surface and probing droplet. Droplets of water spontaneously rolled off of this surface with virtually no surface tilt. Still images of this behavior can be seen in Figure 6a and b, with a representative video of this experiment provided in the Supporting Information (Video S2). Given that fluorodecyl POSS is expected to exhibit a lower surface energy than the particles, it is clear that the favorable built-in geometry of the particles significantly outweighs the differences in surface energy. Scanning electron microscopy (SEM) micrographs of this superhydrophobic film containing the treated fumed silica (Figure S4 of the Supporting Information) reveal a surface with regularly dispersed sub-micrometer features that appear to range from 250 to 500 nm with occasional aggregates ranging from 2 to 10 $\mu$m. AFM analysis provided additional evidence that the majority of the surface consisted of tightly packed sub-micrometer features,

**Figure 7.** From left to right: unmodified precipitated silica, FDec-MCS-treated precipitated silica, and fluorodecyl POSS in water.

although SEM micrographs have proven to be the most reliable source to describe these surfaces. The superhydrophobic behavior of this surface is attributed to the large surface area available between these sub-micrometer features, which allow for a high air−liquid fraction when a water droplet is in contact with it. Interestingly, however, droplets of water pinned on the surface of composites containing prec-FDec-MCS, resulting in extremely high contact angle hysteresis with $\theta_{adv}/\theta_{rec}$= 152.9 ± 2.4°/57.8 ± 10.7°. Large droplets of water remained pinned on this substrate even when the surface was tilted to 90°, shown in Figure 6d. This behavior is consistent with a rough surface that is completely wetted between the interface of the surface and droplet. This behavior is not attributed to residual silanol content interacting with the probing liquid, but is the result of less favorable morphology of silica/fluoroelastomer agglomerates. Compared to composite surfaces containing treated fumed silica, SEM micrographs (Figure S4 of the Supporting Information) also revealed sub-micrometer features, but with a much larger size distribution and a high population of larger features ranging from 5 to 15 $\mu$m. The presence of these larger features is attributed to the large water contact angle hysteresis, presumably caused from contact line pinning and a lower effective air−liquid fraction.

Another demonstration of the superhydrophobicity of the particles is provided by Figure 7, which shows previously hygroscopic silica particles rendered hydrophobic after treatment with fluoroalkyl chlorosilanes. Despite a density of more than 2 g/mL, the treated silica "floated" on the surface of water, even after vigorous shaking. Looking up from beneath the liquid, the "floating" silica appears shiny, the signature of a solid−liquid−air interface present on nearly all superhydrophobic surfaces. The floating state of the silica appears to be indefinite, with samples having thus far retained this property in the laboratory for well over 1 year. Thus, not only was the superhydrophobicity robust, it also was not compromised by long-term proximity to liquid water or high humidity, despite the fact that water clearly can access the hydrophilic sites on the silica particles based on water uptake data. This behavior supports the previous discussion of the wetting properties of the composite containing prec-FDec-MCS. Note that a similarly prepared sample of fluorodecyl POSS has thus far exhibited identical performance.

Thus, as previously mentioned, the built-in geometric characteristics of the treated silica particles, despite having a significant concentration of residual hydrophilic groups on their surfaces, enable superior liquid repelling performance even when used to create stochastically patterned surfaces in elastomeric

composites. This result is in accord with recent reports of superhydrophobicity in polymer nanocomposites containing hydrophilic groups in which the characteristics of the nanoparticles have not been well characterized.[15,16] It also shows that although optimizing both geometry and surface energy is important for the creation of liquid repellant surfaces, the constraints on surface hydrophobicity may be much less than imagined. A more thorough study of the role of fluoroalkylsilane treated silica particles and their geometry in the liquid repellency of elastomeric composites, including repelling low surface tension liquids such as oils, will be the subject of a future publication.

## CONCLUSIONS

Fluoroalkyl-functionalized silica particles have been shown to be highly effective for use in superhydrophobic surfaces. The treatment of dried silica particles with monofunctional chlorosilanes in the presence of preadsorbed dimethylamine was shown to provide the highest grafting densities and lowest effective surface energies. Confirmation of covalent attachment was accomplished via FT-IR spectroscopy, while both elemental analysis and thermogravimetric analysis showed a generally constant grafting density for the precipitated silica regardless of grafted alkyl chain length, with a decreasing grafting density for the fumed silica, with increasing grafted chain length. Both fumed and precipitated silica surfaces appeared to have significant amounts of residual silanol groups, with the precipitated silica showing much greater levels, as expected. The precipitated silica surface also appeared to retain more contaminants. The grafting density and apparent surface energy were consistent with a reasonable coverage of hydrophobic groups, though geometrical parameter estimation indicated that the coating layers were likely to be only 1−2 molecular layers thick and disorganized. Water uptake data showed that, for both types of silica, residual silanols were accessible to ambient humidity. Despite the fact that the surfaces of these particles retained some accessible hydrophilic groups, exposure tests with liquid water revealed them to exhibit similar performance to more ideal hydrophobic surfaces, such as fluorodecyl POSS, with no loss in robustness or durability of liquid repellency on long-term exposure to liquid water. Elastomeric composites made with the treated particles resulted in rough surfaces with static contact angles above 150°. However, under the present deposition conditions, composites containing fumed silica particles treated with FDec-MCS exhibited advancing and receding contact angles above 150°, indicating the production of a stable composite solid−liquid−air interface, while composites containing precipitated silica particles pinned on substrates indicating that a composite interface was not produced. These results combined with SEM analysis indicate that, for liquid repellency of stochastic composite surfaces, favorable geometrical characteristics likely outweigh less than ideal surface characteristics in determining performance. A future publication will elucidate the surface morphology produced from different silica types and deposition methods, and the subsequent ability to produce composite solid−liquid−air interfaces with low surface tension liquids.

## ASSOCIATED CONTENT

**Supporting Information.** Additional tables, figures, videos, and discussion. This material is available free of charge via the Internet at http://pubs.acs.org.

## ACKNOWLEDGMENT

We gratefully acknowledge the Air Force Office of Scientific Research and the Air Force Research Laboratory, Propulsion Directorate for financial support. We would also like to thank Ms. Hong Phan and Ms. Marietta Fernandez for assistance in collecting physisorption data.

## REFERENCES

(1) Feng, X.; Jiang, L. *Adv. Mater.* **2006**, *18*, 3063–3078.
(2) Roach, P.; Shirtcliffe, N. J.; Newton, M. I. *Soft Matter* **2008**, *4*, 224–240.
(3) Zhang, X.; Shi, F.; Niu, J.; Jiang, Y.; Wang, Z. *J. Mater. Chem.* **2008**, *18*, 621–633.
(4) Nosonovsky, M.; Bhushan, B. *Curr. Opin. Colloid Interface Sci.* **2009**, *14*, 270–280.
(5) Gao, L.; McCarthy, T. J. *Langmuir* **2009**, *25*, 14105–14115.
(6) Chhatre, S. S.; Choi, W.; Tuteja, A.; Park, K.-C.; Mabry, J. M.; McKinley, G. H.; Cohen, R. E. *Langmuir* **2010**, *26*, 4027–4035.
(7) Bhushan, B.; Jung, Y. C. *Prog. Mater Sci.* **2011**, *56*, 1–108.
(8) Tsujii, K.; Yamamoto, T.; Onda, T.; Shibuichi, S. *Angew. Chem. Int. Ed* **1997**, *36*, 1011–1012.
(9) Shibuichi, S.; Yamamoto, T.; Onda, T.; Tsujii, K. *J. Colloid Interface Sci.* **1998**, *208*, 287–294.
(10) Cao, L.; Price, T. P.; Weiss, M.; Gao, D. *Langmuir* **2008**, *24*, 1640–1643.
(11) Kumar, R. T. R.; Mogensen, K. B.; Bøggild, P. *J. Phys. Chem. C* **2010**, *114*, 2936–2940.
(12) Guo, M.; Ding, B.; Li, X.; Wang, X.; Yu, J.; Wang, M. *J. Phys. Chem. C* **2010**, *114*, 916–921.
(13) Tuteja, A.; Choi, W.; Mabry, J. M.; McKinley, G. H.; Cohen, R. E. *Proc. Natl. Acad. Sci. U.S.A.* **2008**, *105*, 18200–18205.
(14) Tuteja, A.; Choi, W.; Minglin, M.; Mabry, J. M.; Mazzella, S. A.; Rutledge, G. C.; McKinley, G. H.; R.E., C. *Science* **2007**, *318*, 1618–1622.
(15) Manoudis, P. N.; Karapanagiotis, I.; Tsakalof, A.; Zuburtikudis, I.; Panayiotountheses, C. *Langmuir* **2008**, *24*, 11225–11232.
(16) Steele, A.; Bayer, I.; Loth, E. *Nano Lett.* **2009**, *9*, 501–505.
(17) Yang, J.; Zhang, Z.; Men, X.; Xu, X.; Zhu, X. *New J. Chem.* **2011**, *35*, 576–580.
(18) Hsieh, C.-T.; Wu, F.-L.; Chen, W.-Y. *Mater. Chem. Phys.* **2010**, *121*, 14–21.
(19) Chhatre, S. S.; Tuteja, A.; Choi, W.; Revaux, A.; Smith, D.; Mabry, J. M.; McKinley, G. H.; Cohen, R. E. *Langmuir* **2009**, *25*, 13625–13632.
(20) Choi, B. W.; Tuteja, A.; Chhatre, S.; Mabry, J. M.; Cohen, R.; McKinley, G. H. *Adv. Mater.* **2009**, *21*, 2190–2195.
(21) Darmanin, T.; Guittard, F. *J. Colloid Interface Sci.* **2009**, *335*, 146–149.
(22) Li, H.; Wang, X.; Song, Y.; Liu, Y.; Li, Q.; Jiang, L.; Zhu, D. *Angew. Chem., Int. Ed.* **2001**, *40*, 1743–1746.
(23) Pickering, J. A. U.S. Patent 7,252,885, Aug 7, 2007.
(24) Coggio, W. D. U.S. Patent 7,473,462, Jan 6, 2009.
(25) Bravo, J.; Zhai, L.; Wu, Z.; Cohen, R. E.; Rubner, M. F. *Langmuir* **2007**, *23*, 7293–7298.
(26) Voort, P. V. D.; Vansant, E. F. *J. Liq. Chromatogr. Relat. Technol.* **1996**, *19*, 2723–2752.
(27) Buszewski, B.; Jezierska, M.; Wełniak, M.; Berek, D. *J. High Resolut. Chromatogr.* **1998**, *21*, 267–281.
(28) Sayari, A.; Hamoudi, S. *Chem. Mater.* **2001**, *13*, 3151–3168.
(29) Zhang, W. *J. Fluorine Chem.* **2008**, *129*, 910–919.
(30) Fields, J. T.; Garton, A. *Polym. Compos.* **1996**, *17*, 242–250.
(31) Berendsen, G. E.; Pikaart, K. A.; Galan, L. D.; Olieman, C. *Anal. Chem.* **1980**, *52*, 1990–1993.
(32) Roshchina, T. M.; Shoniya, N. K.; Nikol'skaya, A. B.; Lagutova, M. S.; Fadeev, A. Y. *Prot. Met. Phys. Chem. Surf.* **2009**, *45*, 152–157.
(33) Monde, T.; Nakayama, N.; Yano, K.; Yoko, T.; Konakahara, T. *J. Colloid Interface Sci.* **1997**, *185*, 111–118.

(34) Kamiusuki, T.; Monde, T.; Yano, K.; Yoko, T.; Konakahara, T. *Chromatographia* **1999**, *49*, 649–656.
(35) Xue, L.; Li, J.; Fu, J.; Han, Y. *Colloids Surf., A* **2009**, *338*, 15–19.
(36) Sheen, Y.-C.; Huang, Y.-C.; Liao, C.-S.; Chou, H.-Y.; Chang, F.-C. *J. Polym. Sci., Part B: Polym. Phys.* **2008**, *46*, 1984–1990.
(37) García, N.; Benito, E.; Guzmán, J.; Tiemblo, P. *J. Am. Chem. Soc.* **2007**, *129*, 5052–5060.
(38) Boksányi, L.; Liardon, O.; Kováts, E. s. *Adv. Colloid Interface Sci.* **1976**, *6*, 95–137.
(39) Gallas, J. P.; Lavalley, J. C.; Burneau, A.; Barres, O. *Langmuir* **1991**, *7*, 1235–1240.
(40) Chuang, I.-S.; Maciel, G. E. *J. Phys. Chem. B* **1997**, *101*, 3052–3064.
(41) Berendsen, G. E.; De Galan, L. *J. Liq. Chromatogr.* **1978**, *1*, 403–426.
(42) Roshchina, T. M.; Shonia, N. K.; Kazmina, A. A.; Gurevich, K. B.; Fadeev, A. Y. *J. Chromatogr. A* **2001**, *931*, 119–127.
(43) Scully, N. M.; Healy, L. O.; O'Mahony, T.; Glennon, J. D.; Dietrich, B.; Albert, K. *J. Chromatogr. A* **2008**, *1191*, 99–107.
(44) Buszewski, B.; Nondek, L.; Jurášek, A.; Berek, D. *Chromatographia* **1987**, *23*, 442–446.
(45) Berendsen, G. E.; De, G. L. *J. Liq. Chromatogr.* **1978**, *1*, 561–586.
(46) Bernardoni, F.; Kouba, M.; Fadeev, A. Y. *Chem. Mater.* **2008**, *20*, 382–387.
(47) Mabry, J. M.; Vij, A.; Iacono, S. T.; Viers, B. D. *Angew. Chem. Int. Ed* **2008**, *47*, 4137–4140.
(48) Sindorf, D. W.; Maciel, G. E. *J. Phys. Chem.* **1982**, *86*, 5208–5219.
(49) Brunauer, S.; Emmett, P. H.; Teller, E. *J. Am. Chem. Soc.* **1938**, *60*, 309–319.
(50) Tripp, C. P.; Veregin, R. P. N.; Hair, M. L. *Langmuir* **1993**, *9*, 3518–3522.
(51) Blitz, J. P.; Murthy, R. S. S.; Leyden, D. E. *J. Colloid Interface Sci.* **1988**, *121*, 63–69.
(52) Hair, M. L.; Tripp, C. P. *Colloids Surf., A* **1995**, *105*, 95–103.
(53) Fadeev, A. Y.; Kazakevich, Y. V. *Langmuir* **2002**, *18*, 2665–2672.
(54) Fadeev, A. Y.; McCarthy, T. J. *Langmuir* **2000**, *16*, 7268–7274.
(55) Genzer, J.; Efimenko, K.; Fischer, D. A. *Langmuir* **2002**, *18*, 9307–9311.
(56) Blitz, J. P.; Murthy, R. S. S.; Leyden, D. E. *J. Colloid Interface Sci.* **1988**, *126*, 387–392.
(57) Tripp, C. P.; Hair, M. L. *J. Phys. Chem.* **1993**, *97*, 5693–5698.
(58) Bogart, G. R.; Leyden, D. E. *J. Colloid Interface Sci.* **1994**, *167*, 27–34.
(59) Staszczuk, P.; Buszewski, B. *Chromatographia* **1988**, *25*, 881–886.
(60) Roshchina, T. M.; Gurevich, K. B.; Fadeev, A. Y.; Astakhov, A. L.; Lisichkin, G. V. *J. Chromatogr. A* **1999**, *844*, 225–237.
(61) Kazakevich, Y. V.; Fadeev, A. Y. *Langmuir* **2002**, *18*, 3117–3122.
(62) A TGA plot containing curves for all samples can be found in the Supporting Information in Figure S4.
(63) Sneh, O.; George, S. M. *J. Phys. Chem.* **1995**, *99*, 4639–4647.
(64) Wesson, S. P.; Vajo, J. J. *Adv. Colloid Interface Sci.* **1998**, *76−77*, 107–135.
(65) Visintin, P. M.; Carbonell, R. G.; Cynthia, K, S.; DeSimone, J. M. *Langmuir* **2005**, *21*, 4816–4823.
(66) Bicerano, J. *Prediction of Polymer Properties*, 3rd ed.; Marcel Dekker, Inc.: New York, 2002; p 756.
(67) Spin-coated from 10 wt % suspensions at 900 rpm for 30 s.
(68) Gao, L.; McCarthy, T. J. *Langmuir* **2007**, *23*, 10445–10447.
(69) Aussillous, P.; Quéré, D. *Nature* **2001**, *411*, 924–927.